

Increased sensitivity to radiochemotherapy in IDH1 mutant glioblastoma as demonstrated by serial quantitative MR volumetry

Anh N. Tran, Albert Lai, Sichen Li, Whitney B. Pope, Stephanie Teixeira, Robert J. Harris, Davis C. Woodworth, Phioanh L. Nghiemphu, Timothy F. Cloughesy, and Benjamin M. Ellingson

Duke-National University of Singapore Graduate Medical School, 8 College Road, Singapore (A.N.T.); Department of Radiological Sciences, David Geffen School of Medicine, University of California Los Angeles, Los Angeles, California (A.T., W.B.P., S.T., R.J.H., D.C.W., P.L.N., B.M.E.); Department of Neurology, David Geffen School of Medicine, University of California Los Angeles, Los Angeles, California (A.N.T., A.L., S.L., P.L.N., T.F.C.); Department of Biomedical Physics, David Geffen School of Medicine, University of California Los Angeles, Los Angeles, California (R.J.H., D.C.W., B.M.E.); Department of Bioengineering, David Geffen School of Medicine, University of California Los Angeles, Los Angeles, California (B.M.E.)

Corresponding author: Benjamin M. Ellingson, PhD, Assistant Professor of Radiology, Biomedical Physics, and Bioengineering, Department of Radiological Sciences, David Geffen School of Medicine, University of California – Los Angeles, 924 Westwood Blvd, Suite 615, Los Angeles, CA 90024 (bellingson@mednet.ucla.edu).

Background. *Isocitrate dehydrogenase 1* (IDH1) mutations have been linked to favorable outcomes in patients with glioblastoma multiforme (GBM). Recent in vitro experiments suggest that *IDH1* mutation sensitizes tumors to radiation damage. We hypothesized that radiographic treatment response would be significantly different between *IDH1* mutant versus wild-type GBMs after radiotherapy (RT) and concurrent temozolomide (TMZ).

Methods. A total of 39 newly diagnosed GBM patients with known *IDH1* mutational status (10 *IDH1* mutants), who followed standard therapy and had regular post-contrast T1W (T1+C) and T2W/ fluid-attenuated inversion recovery (FLAIR) images in the 6-month period after starting RT, were enrolled. The volume of contrast-enhancing and FLAIR hyperintensity were calculated from each scan. Linear and polynomial regression techniques were used to estimate the rate of change and temporal patterns in tumor volumes.

Results. *IDH1* mutant GBMs demonstrated a favorable response to RT/TMZ in the study period, as demonstrated by 10 of 10 mutants showing radiographic response (decreasing V_{T1+C}), compared with 13 of 29 wild-types ($P < .001$). During the study period, V_{T1+C} and V_{FLAIR} changed at -3.6% per week and $+0.6\%$ per week in *IDH1* mutant tumors, respectively, as compared with $+0.8\%$ per week and $+5.2\%$ per week in *IDH1* wild-type tumors ($P = .0076$ and $P = .0118$, respectively). Amongst the radiographic responders, *IDH1* mutant GBMs still demonstrated significant progression-free and overall survival benefit. Aggregated tumor kinetics by group showed significant lower rate in *IDH1* mutant GBMs in specific periods: >105 days for V_{FLAIR} and 95–120 and >150 days for V_{T1+C} from starting RT/TMZ.

Conclusions. The current study supports the hypothesis that *IDH1* mutant GBMs are more sensitive to radiochemotherapy than *IDH1* wild-type GBMs.

Keywords: glioblastoma, IDH1 mutation, MRI, radiochemotherapy, volumetry.

Glioblastoma (GBM) is the most common and aggressive form of primary malignant brain tumor and is characterized by genetic instability, intratumoral histopathological variability, and unpredictable clinical behavior. In the recent years, there has been a concerted effort to classify the molecular and genetic variations of GBM with the eventual goal of personalized medicine using targeted, tumor-specific therapy. In 2008, a genome-wide somatic mutational analysis of GBM revealed a subset of an isocitrate dehydrogenase 1 (*IDH1*) mutation at codon R132.¹ Subsequently,

IDH1 mutation was found in all subtypes of gliomas, with the exception of primary GBMs (5%–8%).^{2,3} In these studies, $>90\%$ of the *IDH1* mutations were heterogenous single-base transition substitutions of arginine for histidine ($IDH1^{R132H}$).^{2,3} Evidence from patient demographics, histologic, radiographic, genomic, epigenetic, and transcriptional characteristics suggests that GBMs with *IDH1* mutation represent a distinct disease entity with a completely different clinical behavior⁴ having the tendency to emerge in the frontal lobes in younger individuals⁵ and having

Received 28 May 2013; accepted 29 September 2013

© The Author(s) 2013. Published by Oxford University Press on behalf of the Society for Neuro-Oncology. All rights reserved.
For permissions, please e-mail: journals.permissions@oup.com.

significantly longer progression-free survival (PFS) and overall survival (OS).^{1,2,6}

The precise mechanism behind the improved survival of *IDH1* mutant GBMs remains unclear; however, recent studies have suggested that increased sensitivity to oxidative damage may play a pivotal role. The *IDH1* enzyme catalyzes the conversion of isocitrate to α -ketoglutarate, thereby reducing NADP to NADPH. Zhao et al⁷ recently showed that mutation of *IDH1* can impair the enzyme's activity, which in turn reduces the amount of NADPH available for protection from oxidative damage. Alternatively, Dang et al⁸ demonstrated that the *IDH1*^{R132H} protein may increase enzyme activity, leading to the reduction of α -ketoglutarate to 2-hydroxyglutarate and the oxidation of NADPH to NADP, further reducing the levels of NADPH and making the cell even more susceptible to oxidative damage. Regardless of change in enzyme activity, both of these studies suggest that the downstream effects result in increased susceptibility to oxidative damage. Consistent with this hypothesis, Li et al⁹ recently showed that overexpression of the *IDH1*^{R132H} protein in glioma cell lines increased their sensitivity to radiation damage since radiation exposure is thought to induce cell death through perturbations in intracellular metabolic oxidation/reduction reactions.¹⁰

The purpose of the current study was to compare differences in tumor growth rates between human *IDH1* mutant to *IDH1* wild-type glioblastomas after the start of standard radiochemotherapy using serial volumetric analysis of anatomic magnetic resonance images.

Materials and Methods

Patients

All patients participating in this study signed an institutional review board-approved informed consent. In this study, a total of 39 participants (*IDH1* mutants, $n = 10$; *IDH1* wild-type, $n = 29$) were selected from previously published cohorts of nearly 400 participants^{4,11} with the following criteria: (i) newly diagnosed GBM, (ii) surgery followed by radiotherapy (RT) (6000 cGy) and concurrent temozolomide (TMZ), (iii) had *IDH1* mutation status sequenced from frozen section samples at initial diagnosis, (iv) had contrast-enhancing tumor in post-contrast T1-weighted images (T1+C), and (v) had regular follow-up MR images (T1+C and fluid-attenuated inversion recovery [FLAIR] or T2-weighted images) within 6 months after starting RT. To the best of our knowledge, participants were on a constant level of steroids during imaging evaluation. In order to assess the response to radiochemotherapy exclusively, participants who were clinically diagnosed with tumor progression within the study period were removed from the study at the time of progression due to the subsequent change in their treatment plan (eg, additional resection, bevacizumab, or enrollment in a clinical trial). A higher proportion of *IDH1* mutant glioblastomas was selected from our database to increase statistical power, since *IDH1* mutation only occurs in a small subset of primary glioblastoma (5%–8%).^{2,3} Postsurgical, posttreatment scans obtained ~2–4 weeks after completion of RT were used as the baseline for subsequent analyses. Postsurgical, pre-RT scans were not included due to possible edema, swelling, and blood products after surgery that may contaminate estimates of initial tumor burden. All participants were diagnosed between November 2004 and October 2011. Table 1 outlines additional characteristics in our participant population.

Magnetic Resonance Imaging

Magnetic resonance imaging (MRI) data were collected on either a 1.5T or 3T MR imaging scanner Siemens Healthcare (Erlangen, Germany). Standard

Table 1. Participant characteristics and follow-up periods

	IDH1 Mutant ($n = 10$)	IDH1 Wild-type ($n = 29$)
Surgical resection		
Biopsy	1 (10%)	3 (10%)
Gross total	6 (60%)	18 (62%)
Subtotal	3 (30%)	8 (28%)
Diagnosed time	11/2004–04/2011	08/2006–10/2011
Age in years (range)	48.5 (31–61)	57 (23–78)
Days from surgery to RT	37 days	31 days
Number of scans	2.8	3.3
Number of days followed up (range)	151.7 days (92–184)	143.7 days (51–192)
Preoperative volume		
V_{T1+C}	8.8 ± 3.4 cc	20.0 ± 3.0 cc
V_{FLAIR}	78.9 ± 21.9 cc	99.5 ± 11.5 cc
MGMT methylation status		
Methylated	5 (50%)	12 (41%)
Unmethylated	3 (30%)	15 (52%)
No result	2 (20%)	2 (7%)

anatomic MR imaging consisted of clinical T2-weighted fast spin-echo or FLAIR images and gadolinium-diethylene-triamine penta-acetic acid (Magnevist; Berlex; 0.1 mmol/kg) or gadobenate dimeglumine (MultiHance; Bracco; 0.1 mmol/kg) enhanced T1-weighted images (ie, T1+C). All images were 3- to 5-mm thick with a 0 to 1 mm intersection gap. Each participant received consistent MR data acquisition protocols to baseline scans during subsequent follow-ups in order to reduce variability that may have been due to differences in MR acquisition parameters.

MR Volumetry

Regions of interest were segmented using a semiautomated procedure coded in AFNI (<http://afni.nimh.nih.gov/afni>). Briefly, the general regions of tumor on T2/FLAIR and T1+C images were first defined manually. Then, T2/FLAIR and T1+C images were thresholded by using an empirical threshold. Finally, the resulting masks were edited manually to exclude obvious errors. Only tumor near the original lesion site was contoured to better estimate the response to treatment since satellite lesions may have grown outside the original RT field. Contrast-enhancing tumor volume, V_{T1+C} , and T2/FLAIR hyperintense volume, V_{FLAIR} , were calculated for each time point using the respective image resolution. All tumor contours were verified by an expert, board-certified neuroradiologist (W.B.P.).

Temporal Trends Using Local Polynomial Regression Fitting

To visualize population-based growth rate of the tumor adjusted to baseline volumes, we performed a local polynomial regression fitting on the percentage change in volume as a function of time with respect to baseline for both *IDH1* mutant and wild-type cases. Data analysis was performed using R version 2.15.2 (The R Foundation for Statistical Computing) using the *ggplot2* package.

Genetic and Methylation Analysis

IDH1 mutation and MGMT methylation statuses were determined from previously published studies.^{4,11} Briefly, for determination of sequence at *IDH1*

residue 132, both Sanger and Sequenom were utilized. All *IDH1*^{R132MUT} were confirmed with both platforms. MGMT methylation status was determined via methylation-specific PCR as described in (cite PMID 23328811).

Definition of Tumor Progression and Survival

Disease progression was defined by modified Levin criteria as described previously.¹² Briefly, tumor recurrence was confirmed using either direct pathological confirmation, 3,4-dihydroxy-6-[¹⁸F]-fluoro-L-phenylalanine (¹⁸F-FDOPA) PET or unequivocal evidence on MRI as indicated by a board-certified neuroradiologist (W.B.P). Unequivocal evidence on MRI was determined by >2 sequential months of increasing contrast enhancement on post-contrast T1-weighted images along with evidence of increasing mass effect. PFS was defined from the time of initial tissue diagnosis to the first posttreatment scan that showed disease progression. OS was recorded from the time of initial diagnosis until death. Survival comparisons were performed by log-rank analysis on Kaplan–Meier data. All statistical analysis was performed using GraphPad Prism version 5 for Mac(GraphPad Software).

Results

Of the 39 participants evaluated in the current study, 2 (1 *IDH1* wild-type and 1 *IDH1* mutant) had an additional therapy prior to their first progression and were censored at the time of starting new therapy (2 and 4 months after completion of radiation, respectively). *IDH1* mutant glioblastoma participants tended to be younger compared with wild-type glioblastoma participants (average age 48.5y vs 57y), while the extent of surgical resection was comparable between the 2 groups (60%–62% gross total, 30%–28% subtotal). The average follow-up periods from the start of RT were ~5.1 months for *IDH1* mutant and 4.8 months for *IDH1* wild-type glioblastomas. At the time of diagnosis, average contrast-enhancing tumor volume (V_{T1+C}) was 8.8cc for *IDH1* mutant and 20cc for *IDH1* wild-type tumors (*t* test, $P < .0001$), while the average T2/FLAIR hyperintense volume (V_{FLAIR}) was 78.9cc for *IDH1* mutant and 99.5cc for *IDH1* wild-type tumors (*t* test, $P = .0005$).

IDH1 Mutant Tumors Decrease in Volume After Radiochemotherapy

Fig. 1 shows the typical radiographic response of an *IDH1* mutant and wild-type tumors during the period of evaluation. A significantly larger proportion of *IDH1* mutant GBMs showed a favorable response after RT (100%, 10 of 10) as indicated by a decrease in both contrast-enhancing and T2/FLAIR hyperintense volume compared with *IDH1* wild-type GBMs (44.8%, 13 of 29; binomial test, $P < .001$). Linear regression of temporal trends in volume measurements after completion of radiochemotherapy indicated that contrast-enhancing *IDH1* mutant GBMs decreased in volume at ~3.6% per week, which was significantly different than *IDH1* wild-type GBMs that increased at a rate of 0.8% per week (Fig. 3, Mann-Whitney test, $P = .0076$). T2/FLAIR hyperintense lesion growth rates showed similar trends, indicating an average increase in volume after RT of 0.6% per week in *IDH1* mutant glioblastoma and an increase in volume of 5.2% per week in *IDH1* wild-type tumors (Fig. 3, Mann-Whitney test, $P = .0118$).

Further characterization of differences in tumor growth kinetics between *IDH1* mutant and wild-type tumors was performed using a local polynomial regression model (Fig. 2). Differences in tumor

growth kinetics were observed in both contrast-enhancing and T2/FLAIR hyperintense lesions for *IDH1* mutant and wild-type tumors. Specifically, we observed a consistent overall decrease in tumor volume in *IDH1* mutant tumors after completion of radiochemotherapy, whereas population-based growth kinetic trends for *IDH1* wild-type tumors suggested a general increase in lesion volume after therapy. T2/FLAIR hyperintense tumor growth kinetic trends were significantly different after day 105 (period *a*) from starting RT. Interestingly, the aggregated trend in tumor growth kinetics for contrast-enhancing lesions was significantly different between *IDH1* mutant and wild-type tumors at 2 specific periods after completion of radiochemotherapy: between days 95–120 (period *b*) and beyond 150 (period *c*) days posttherapy.

IDH1 Mutant Glioblastomas Show a Progression-free Survival Benefit from Radiochemotherapy

Since our criteria for treatment response in this study were based on radiographic contrast-enhancing volumes at the site of original tumor, 9 of 16 nonresponders and 3 of 23 responders (all *IDH1* wild-type) progressed clinically during the study duration.

To test whether *IDH1* mutant glioblastomas show a PFS benefit from RT and concurrent TMZ, we performed log-rank analysis on Kaplan–Meier data. Results suggested that *IDH1* mutant glioblastomas had a significantly longer PFS compared with *IDH1* wild-type tumors (Fig. 4A; *IDH1* mutant median PFS = 72.1m vs *IDH1* wild-type median PFS = 8.1m; log-rank test, $P = .0004$). This trend was also evident when examining OS (Fig. 4D; *IDH1* mutant median OS = 72.1m vs *IDH1* wild-type median OS = 18.6m; log-rank test, $P = .006$); however, variability in treatment paradigms after recurrence may have further influenced these results.

The initial tumor growth kinetics after completion of radiochemotherapy were then used to predict PFS and OS in *IDH1* mutant and wild-type tumors (Fig. 4B and C). Results suggest tumors demonstrating a negative rate of change in V_{T1+C} after completion of radiochemotherapy, indicative of a positive response to therapy, had a longer PFS (Fig. 4B: radiographic responders median PFS = 18.6m vs radiographic nonresponders median PFS = 6.7m; log-rank test, $P < .0001$) and OS (Fig. 4E: radiographic responders median OS = 72.1m vs radiographic nonresponders median OS = 17.2m; log-rank test, $P = .0056$). When we only looked at the V_{T1+C} responders, *IDH1* mutation status still conferred a significant PFS (Fig. 4C: log-rank test, $P = .014$) and OS (Fig. 4F: log-rank, $P = .045$) benefit. Additionally, rates of change in T2/FLAIR hyperintense lesions were not predictive of PFS (log-rank test, $P = .1210$) or OS (log-rank test, $P = .3230$) (not shown).

Discussion

To the best of our knowledge, this is the first study to explore the treatment response in human *IDH1* mutant glioblastomas to the standard treatment regime. Consistent with recent in vitro results from Li et al⁹ and clinical data from van den Bent et al,¹³ results from the current study support the hypothesis that *IDH1* mutated malignant gliomas are more sensitive to radiochemotherapy. In particular, results clearly demonstrate that the contrast-enhancing lesion continues to decrease in volume after completion of RT while on concurrent chemotherapy in 100% of *IDH1* mutant glioblastomas examined, whereas only around

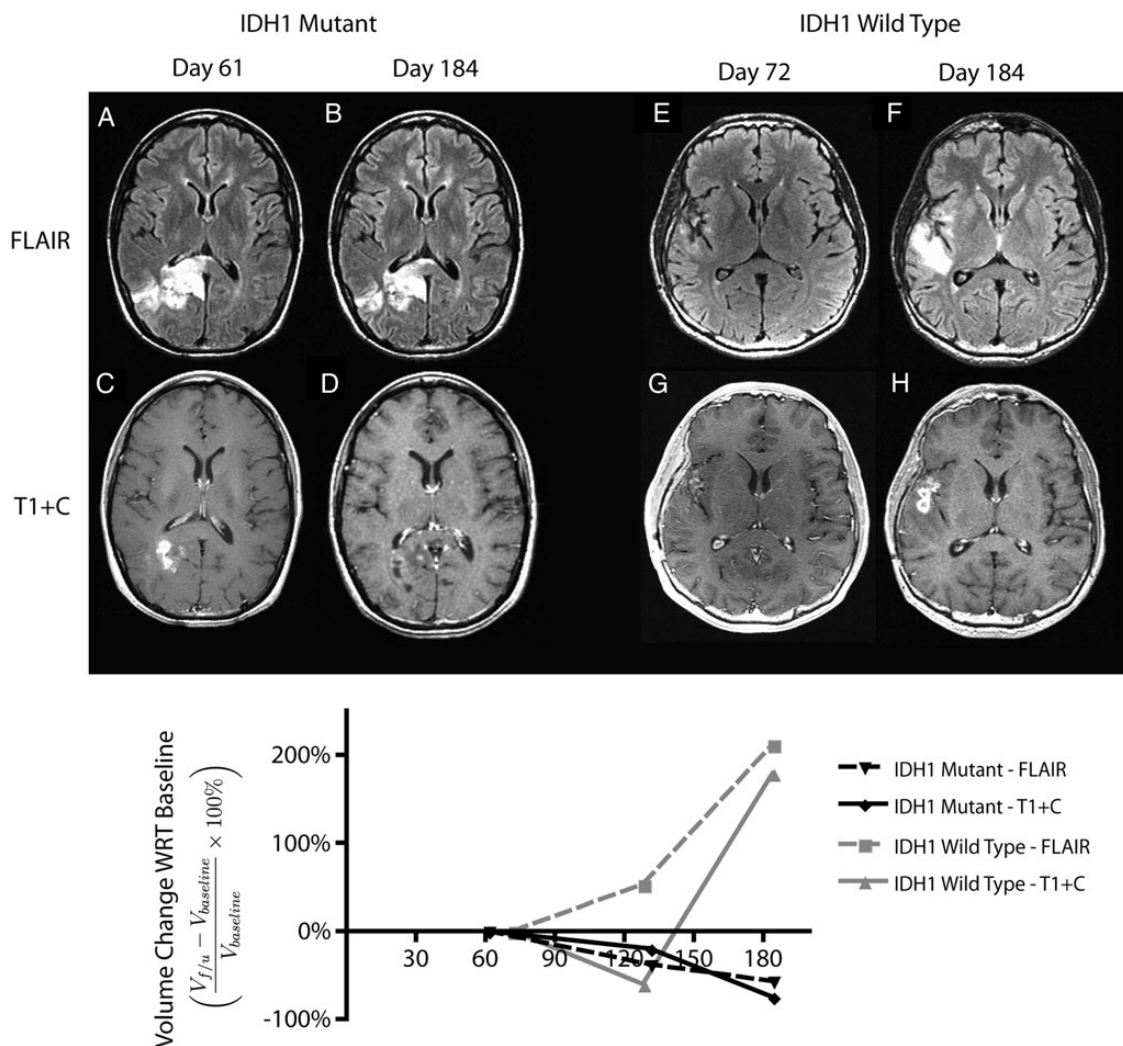


Fig. 1. Radiographic changes and serial volumetric analysis of a responder and nonresponder to radiochemotherapy regime. All MR images were dated with regard to the start date of radiotherapy. Baseline volumes of T2/FLAIR hyperintense region (V_{FLAIR}) and contrast-enhancing tumor (V_{T1+C}) were measured from the first scans postradiotherapy (A, B: IDH1 mutant case and E, F: IDH1 wild-type case). Tumor kinetics were estimated by measuring the relative changes of the region of interest in subsequent scans (C, D: IDH1 mutant case and G, H: IDH1 wild-type case) with regard to the baseline volume. I: The relative volumes were presented as a function of time. Dashed lines denote the trend in V_{FLAIR} . Solid lines denote the trend in V_{T1+C} .

45% of *IDH1* wild-type tumors responded favorably in the same period.

IDH1 Mutant GBMs Demonstrated a Distinct Response Profile to Radiochemotherapy

The *IDH1* mutant cases showed stable T2/FLAIR lesions and steadily decreasing contrast-enhancing tumors (Fig. 2). The difference is apparent when compared with the rapidly increasing trend of both T2/FLAIR lesions and contrast-enhancing tumors in *IDH1* wild-type cases (Fig. 2). Analysis of individual tumor kinetics revealed that *IDH1* mutant tumors had very similar responses in both T2/FLAIR and contrast-enhancing volumes, while *IDH1* wild-type demonstrated large variable responses (Fig. 2 and 3). These observed effects are likely caused by the irradiation damage and initial response to TMZ. In fact, survival analysis showed a strong correlation between PFS and the initial response in contrast-enhancing

lesions (Fig. 4B, log-rank test, $P < .001$) as expected. The presence of *IDH1*^{R132H} mutation is associated with better PFS and OS even amongst the responders (Fig. 4A–F). This result supports our hypothesis that *IDH1*^{R132H} mutation correlates with better response to radiochemotherapy.

The mechanism for increased sensitivity to cytotoxic therapies in *IDH1* mutant glioblastoma during this period (immediate post-RT with concurrent chemotherapy) is likely related to the increased radiation sensitivity. *IDH1*^{R132H} mutation was shown to correlate with diminished NADPH production in situ in glioblastoma by a recent metabolic mapping study.¹⁴ Depletion in NADPH levels can cause the cells to have decreased buffering of reactive oxygen species (ROS) and sensitize them to radiation damage. *IDH1* enzyme plays an important role in the cells in maintaining the NADPH levels to buffer against ROS. In recent studies, an increase in radiation sensitivity was observed when mitochondrial *IDH1* activity was suppressed via small interfering RNA¹⁵ or feedback

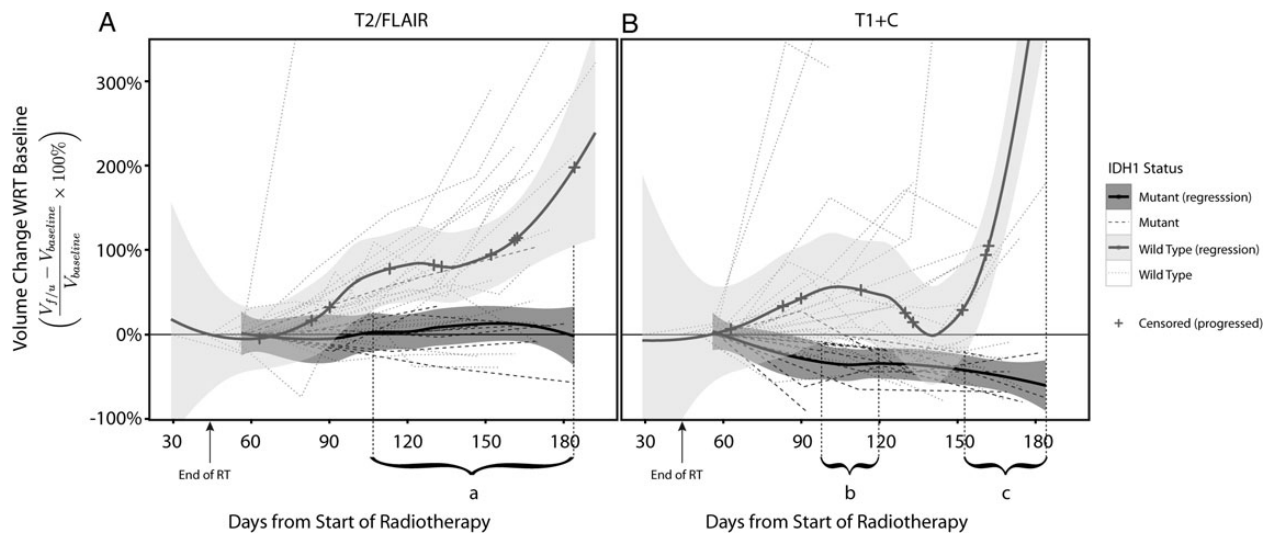


Fig. 2. Temporal trends of (A) T2/FLAIR hyperintense volume and (B) contrast-enhancing volume in IDH1 mutant versus wild-type glioblastoma. Time series of relative change in V_{FLAIR} and V_{T1+C} volume with regard to baseline scans of each participant were presented. Local polynomial regression trend lines were fitted to IDH1 mutant and wild-type groups separately, and presented with 95% standard error bands. The cross marks on the trend line denoted a participant who had progressed ($n = 13$ IDH1 wild-type). Periods which IDH1 wild-type had significantly higher growth rate compared with IDH1 mutant are (a) V_{FLAIR} rate from days 105–180, V_{T1+C} rate from (b) days 95–120 and (c) day 150 onwards.

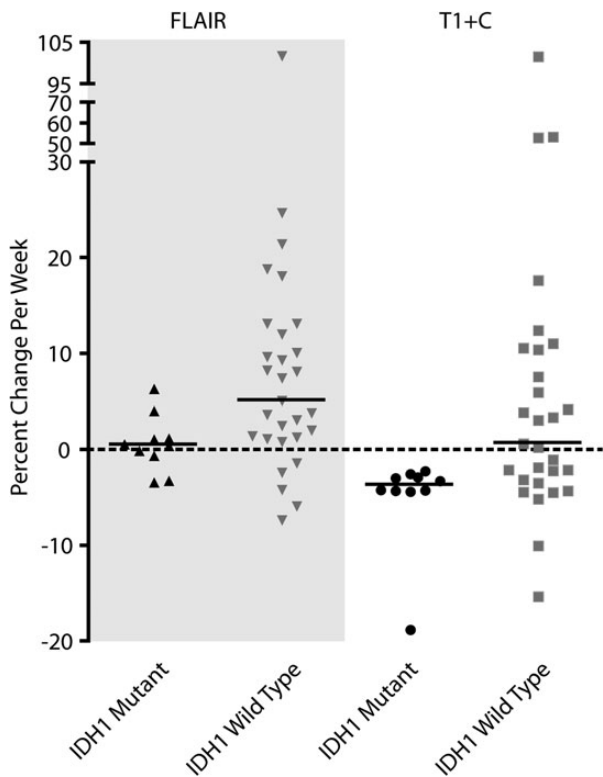


Fig. 3. Tumor growth rate (in percentage per week) for T2/FLAIR hyperintense region V_{FLAIR} and contrast-enhancing volume V_{T1+C} . Results suggest a significant higher growth rate of V_{FLAIR} (Mann-Whitney test, $P = .0118$) and V_{T1+C} (Mann-Whitney test, $P = .0076$) in IDH1 wild-type glioblastomas as compared with IDH1 mutant glioblastomas. Medians of the rates are presented.

inhibition from oxalomalate.¹⁶ The presence of IDH1^{R132H} protein was shown to inhibit the function of normal IDH1 catalytic activity.⁷ IDH1^{R132H} was also found to catalyze the reaction to convert α -ketoglutarate to 2-hydroxyglutarate, resulting in increased ROS levels.⁸ In vitro studies showed that overexpression of IDH1^{R132H} protein in U87MG glioblastoma cell lines were also found to increase radiation sensitivity.⁹ Additionally, recent metabolomic data using high-resolution magic spinning angle MR spectroscopy applied to ex vivo IDH1 mutant tumor tissue has also measured an increase in glutathione,¹⁷ which may further influence sensitivity to IDH1 mutants. Although evidence from various studies suggests that IDH1^{R132H} radiation sensitizing effect is responsible for the observed therapeutic response in vivo, we cannot definitively exclude the effects from the concurrent TMZ treatment. Definitive clinical evidence on the role of IDH1^{R132H} in RT or TMZ response may be derived from the results of an ongoing randomized prospective trial that compares RT-only with TMZ-only treatments (the EORTC 22033–26033).¹⁸

IDH1 Wild-type GBMs Exhibited Pseudoprogression Growth Pattern During the Period of 3–4 Months Postradiotherapy

Interestingly, the growth rate of wild-type tumors increased initially and then decreased roughly at about day 140 (3–4 months after starting radiation, Fig. 2), which appears to coincide with the commonly reported period of “pseudoprogression,” a phenomenon where a temporary increase in contrast-enhancement is observed that mimics tumor progression but actually relates to a favorable response to therapy. Although this observation could have been artifactual from participants being censored after early progression, closer examination of the data suggested this was not the case. Specifically, the censor points on the plot in Fig. 2 clearly

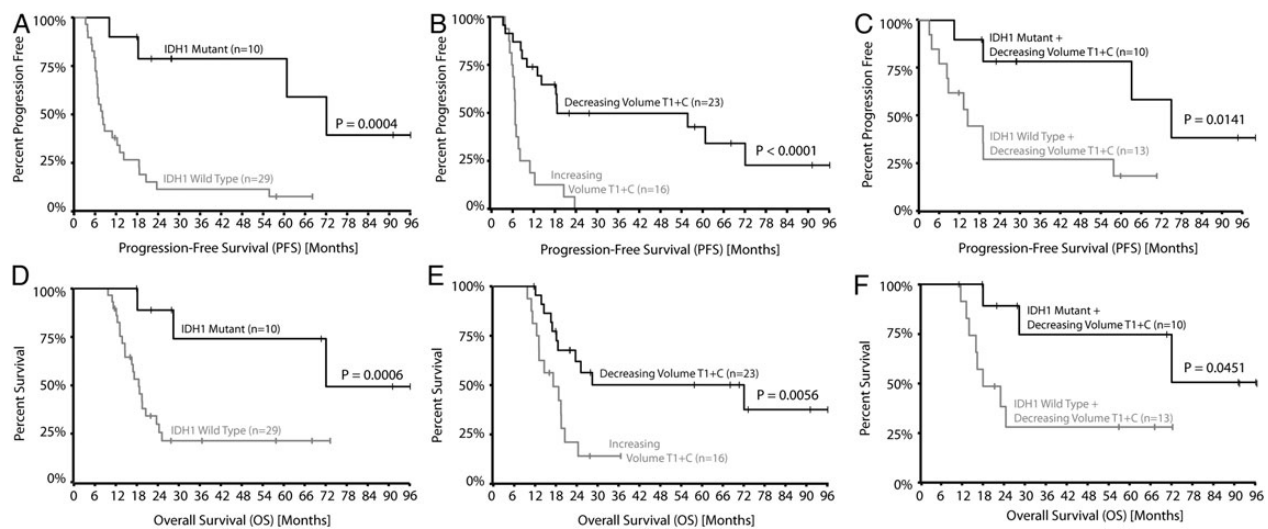


Fig. 4. Kaplan–Meier plots of progression-free survival (PFS) and overall survival (OS) analysis. (A and D) PFS and OS analysis stratified by *IDH1* mutation status showed a significant PFS benefit (mutant median = 72.1m; wild-type median = 8.1m; log-rank test, $P < .001$) and OS benefit (mutant median = 72.1m; wild-type median = 18.6m; log-rank test, $P < .001$) of *IDH1* mutant GBMs. (B and E) PFS and OS analysis stratified by treatment response via V_{T1+C} (using serial MR volumetry analysis) showed significant difference in PFS response (responders median PFS = 18.6m; nonresponders median PFS = 6.7m; log-rank test, $P < .0001$) and OS response (responders median OS = 17.2m; nonresponders median OS = 72.1m; log-rank test, $P = .0056$). (C,F) PFS and OS analysis of V_{T1+C} responders stratified by *IDH1* mutation status showed that even among the responders, *IDH1* mutant GBMs still had significant PFS (mutant median = 72.1m; wild-type median = 14.2m; log-rank test, $P = .0141$) and OS (mutant median = 72.1m; wild-type median = 21.1m; log-rank test, $P = .0451$) advantage. Survival analysis stratified by V_{FLAIR} treatment responses were not significant and not shown here.

show that subjects were censored relatively evenly after therapy. Of the 12 participants who were diagnosed to have progression in our study period, all of them had *IDH1* wild-type genotype. Their *MGMT* promoter methylation statuses were as follows: 5 methylated, 5 unmethylated, and 2 unconfirmed. Four of 6 participants who were diagnosed with progression within the first 6 months postsurgery (roughly 4–5 months since starting RT) had methylated *MGMT* promoter region. Only one of these 6 participants had confirmed unmethylated *MGMT* promoter region. This result is consistent with the association of methylated *MGMT* tumors with pseudoprogression phenomenon in the literature.^{19,20} Further investigation into the roles of other molecular or genetic alterations (eg, *MGMT* promoter methylation) and resulting population-based response to RT are warranted.

Study Limitations

Since the current study was retrospective, MR images used in the current study were not acquired in a prospective, standardized fashion. MR images were acquired at different sites with different acquisition parameters, including differences in field strength (3T and 1.5T), type of gadolinium contrast agent used, differing imaging-section thickness, etc. This lack of standardization may have led to errors in segmentation and volume estimation. Additionally, the small sample size for *IDH1* mutant glioblastomas in the current study ($n = 10$) is a potential limitation; however, newly diagnosed glioblastomas (primary or secondary that escaped early detection) with *IDH1* mutation are extremely rare;^{2,3} thus, despite this potential limitation, response data on these tumor subtypes may be extremely valuable.

Conclusion

The current study suggests *IDH1* mutant glioblastomas are more sensitive to standard radiochemotherapy compared with *IDH1* wild-type glioblastomas, as demonstrated by serial MR volumetry following therapy.

Funding

NIH/NCI R21 CA167354 (BME); UCLA Institute for Molecular Medicine Seed Grant (BME); UCLA Radiology Exploratory Research Grant (BME); University of California Cancer Research Coordinating Committee Grant (BME); ACRIN Young Investigator Initiative Grant (BME); Art of the Brain (TFC); Ziering Family Foundation in memory of Sigi Ziering (TFC); Singleton Family Foundation (TFC); and Clarence Klein Fund for Neuro-Oncology (TFC).

Conflict of interest statement. None declared.

References

- Parsons DW, Jones S, Zhang X, et al. An integrated genomic analysis of human glioblastoma multiforme. *Science*. 2008;321(5897):1807–1812.
- Yan H, Parsons DW, Jin G, et al. *IDH1* and *IDH2* mutations in gliomas. *The New England Journal of Medicine*. 2009;360(8):765–773.
- Balss J, Meyer J, Mueller W, Korshunov A, Hartmann C, von Deimling A. Analysis of the *IDH1* codon 132 mutation in brain tumors. *Acta Neuropathologica*. 2008;116(6):597–602.

4. Lai A, Kharbanda S, Pope WB, et al. Evidence for sequenced molecular evolution of IDH1 mutant glioblastoma from a distinct cell of origin. *J Clin Oncol*. 2011;29(34):4482–4490.
5. Ellingson BM, Lai A, Harris RJ, et al. Probabilistic radiographic atlas of glioblastoma phenotypes. *AJNR. American Journal of Neuroradiology*. 2013;34(3):533–540.
6. Weller M, Felsberg J, Hartmann C, et al. Molecular predictors of progression-free and overall survival in patients with newly diagnosed glioblastoma: a prospective translational study of the German Glioma Network. *J Clin Oncol*. 2009;27(34):5743–5750.
7. Zhao S, Lin Y, Xu W, et al. Glioma-derived mutations in IDH1 dominantly inhibit IDH1 catalytic activity and induce HIF-1 α . *Science*. 2009;324(5924):261–265.
8. Dang L, White DW, Gross S, et al. Cancer-associated IDH1 mutations produce 2-hydroxyglutarate. *Nature*. 2009;462(7274):739–744.
9. Li S, Chou AP, Chen W, et al. Overexpression of isocitrate dehydrogenase mutant proteins renders glioma cells more sensitive to radiation. *Neuro Oncol*. 2013;15(1):57–68.
10. Spitz DR, Azzam EI, Li JJ, Gius D. Metabolic oxidation/reduction reactions and cellular responses to ionizing radiation: a unifying concept in stress response biology. *Cancer Metastasis Rev*. 2004;23(3–4):311–322.
11. Lalezari S, Chou AP, Tran A, et al. Combined analysis of O6-methylguanine-DNA methyltransferase protein expression and promoter methylation provides optimized prognostication of glioblastoma outcome. *Neuro Oncol*. 2013;15(3):370–381.
12. Lai A, Tran A, Nghiemphu PL, et al. Phase II study of bevacizumab plus temozolomide during and after radiation therapy for patients with newly diagnosed glioblastoma multiforme. *J Clin Oncol*. 2011;29(2):142–148.
13. van den Bent MJ, Dubbink HJ, Marie Y, et al. IDH1 and IDH2 mutations are prognostic but not predictive for outcome in anaplastic oligodendroglial tumors: a report of the European Organization for Research and Treatment of Cancer Brain Tumor Group. *Clinical Cancer Research: An Official Journal of the American Association for Cancer Research*. 2010;16(5):1597–1604.
14. Bleeker FE, Atai NA, Lamba S, et al. The prognostic IDH1(R132) mutation is associated with reduced NADP $^{+}$ -dependent IDH activity in glioblastoma. *Acta Neuropathologica*. 2010;119(4):487–494.
15. Lee JH, Kim SY, Kil IS, Park JW. Regulation of ionizing radiation-induced apoptosis by mitochondrial NADP $^{+}$ -dependent isocitrate dehydrogenase. *The Journal of Biological Chemistry*. 2007;282(18):13385–13394.
16. Lee JH, Park JW. Oxalomalate regulates ionizing radiation-induced apoptosis in mice. *Free Radical Biology and Medicine*. 2007;42(1):44–51.
17. Jalbert LE, Elkhaled A, Phillips JJ, Chang SM, Nelson SJ. Image-guided metabolomic analysis of 2-hydroxyglutarate in IDH-mutant gliomas. *Proc Int Soc Magn Reson Med*. 2013;21:510.
18. Musat E, Roelofs E, Bar-Deroma R, et al. Dummy run and conformity indices in the ongoing EORTC low-grade glioma trial 22033–26033: First evaluation of quality of radiotherapy planning. *Radiotherapy and Oncology: Journal of the European Society for Therapeutic Radiology and Oncology*. 2010;95(2):218–224.
19. Brandes AA, Franceschi E, Tosoni A, et al. MGMT promoter methylation status can predict the incidence and outcome of pseudoprogression after concomitant radiochemotherapy in newly diagnosed glioblastoma patients. *J Clin Oncol*. 2008;26(13):2192–2197.
20. Brandsma D, Stalpers L, Taal W, Sminia P, van den Bent MJ. Clinical features, mechanisms, and management of pseudoprogression in malignant gliomas. *The Lancet Oncology*. 2008;9(5):453–461.